Defining pyromes and global syndromes of fire regimes

Sally Archibald[a,b,1], Caroline E. R. Lehmann[c], Jose L. Gómez-Dans[d], and Ross A. Bradstock[e]

[a]Natural Resources and the Environment, Council for Scientific and Industrial Research, Pretoria 0001, South Africa; [b]School of Animal, Plant and Environmental Sciences, University of the Witwatersrand, Johannesburg 2050, South Africa; [c]Department of Biological Sciences, Macquarie University, North Ryde, NSW 2109, Australia; [d]National Centre for Earth Observation and Department of Geography, University College London, London WC1E 6BT, United Kingdom; and [e]Institute for Conservation Biology and Environmental Management, University of Wollongong, Wollongong, NSW 2522, Australia

Edited by James T. Randerson, University of California, Irvine, CA, and accepted by the Editorial Board March 7, 2013 (received for review July 17, 2012)

Fire is a ubiquitous component of the Earth system that is poorly understood. To date, a global-scale understanding of fire is largely limited to the annual extent of burning as detected by satellites. This is problematic because fire is multidimensional, and focus on a single metric belies its complexity and importance within the Earth system. To address this, we identified five key characteristics of fire regimes—size, frequency, intensity, season, and extent—and combined new and existing global datasets to represent each. We assessed how these global fire regime characteristics are related to patterns of climate, vegetation (biomes), and human activity. Cross-correlations demonstrate that only certain combinations of fire characteristics are possible, reflecting fundamental constraints in the types of fire regimes that can exist. A Bayesian clustering algorithm identified five global syndromes of fire regimes, or pyromes. Four pyromes represent distinctions between crown, litter, and grass-fueled fires, and the relationship of these to biomes and climate are not deterministic. Pyromes were partially discriminated on the basis of available moisture and rainfall seasonality. Human impacts also affected pyromes and are globally apparent as the driver of a fifth and unique pyrome that represents human-engineered modifications to fire characteristics. Differing biomes and climates may be represented within the same pyrome, implying that pathways of change in future fire regimes in response to changes in climate and human activity may be difficult to predict.

fire-climate-vegetation feedbacks | energetic constraints | fire intensity | fire return period | fire size

Fires occur with varying regularity and severity across almost every biome on Earth. Like vegetation, the fire that occurs at a point in space is controlled by environmental characteristics, and should change in a predictable manner along environmental gradients. In contrast to vegetation, a definition of global-scale units of fire is lacking.

Fire is often described in terms of a fire regime, which represents a particular combination of fire characteristics, such as frequency, intensity, size, season, type, and extent (1, 2). It describes the repeated pattern of fire at a location in space. Fire regimes were originally used to explain plant responses to fire (such as resprouting or seroteny) (1). However, characterizing fire regimes is also necessary when quantifying emissions from fires (3) and planning fire suppression and control (4), and is particularly important if we hope to predict how patterns of fire might change in response to environmental and human drivers (5, 6). At global scales, fire regimes could be seen as analogous to biomes.

To date, global analyses have used satellite-derived active fire and burned area data to describe the extent, interannual variability, and seasonality of burning (3, 7–9). This has contributed to an emerging global theory of fire that highlights two major energetic controls of burned area: fuel and weather (10–13). Fuel and weather show opposite trends along a productivity gradient: low-productivity environments usually do not produce enough fuel, whereas in high-biomass environments the fuel is usually too wet to burn.

We expect that such energetic considerations should act to constrain other fire characteristics to a greater or lesser extent. For example, fire intensity is strongly determined by the amount of fuel available, whereas fire frequency and fire seasonality might be more closely related to the probability of flammable conditions.

At global scale we also expect to find tradeoffs between fire characteristics, not unlike the ecological tradeoffs identified between plant traits (14) whereby not all combinations are equally probable or even possible. Where fire is frequent (i.e., every 1–3 y), fuel loads capable of producing high-intensity fires would not have enough time to accumulate. Hence, fire frequency and maximum fireline intensity should be negatively related, and we would not expect a fire regime with frequent, high-intensity fires to exist.

Some of the most pressing fire science and management questions concern changes in fire regimes caused by the introduction of invasive species (15), altered ignition patterns (16), or climate change (17). To determine how permanent these changes are and what sorts of fire regimes are emerging in these ecosystems, we need better predictive understanding of relationships with climate, vegetation, and human drivers.

These relationships are difficult to define statistically as a result of feedbacks within the fire–vegetation–climate system. A fire that occurs at a point in space is a product of the vegetation and climate; vegetation is strongly controlled by climate and fire (18, 19); and (over longer time scales) vegetation and fire in turn affect climate through altering fluxes of energy, water, carbon, and the optical and radiative properties of the atmosphere (20, 21). Correlative studies are unsatisfactory because they have to flatten the system by representing one of the elements as a response and the others as drivers.

Process-based models such as coupled climate–vegetation models can represent much of the complexity of the fire–vegetation–climate system. However, their very complexity prevents useful generalization. Plant community ecology and functional ecology (18, 22) have proven useful for understanding global patterns of vegetation. We draw on this rich theory in an analysis of global fire characteristics and their links to vegetation and climate.

Conceptually, global vegetation units (i.e., biomes) are characterized solely by the traits of vegetation (18), and the environmental correlates emerge post hoc and help to explain the boundaries between biomes. Similarly, we identify five key fire regime characteristics that can consistently be quantified at global scales by using remotely sensed imagery. We determine the leading dimensions of variation in fire, and assess which combinations of fire characteristics are more probable. By using clustering analyses, we group regions with similar fire characteristics and identify global units of fire (i.e., pyromes).

Author contributions: S.A., C.E.R.L., and R.A.B. designed research; S.A. and C.E.R.L. performed research; S.A. and J.L.G.-D. contributed new reagents/analytic tools; S.A. and C.E.R.L. analyzed data; and S.A., C.E.R.L., and R.A.B. wrote the paper.

Conflict of interest statement: David Bowman was supervisor and collaborator of C.E.R.L. and is a current collaborator with R.A.B.; William Bond is a current collaborator of S.A. and C.E.R.L.; and Simon Levin is a current collaborator of S.A.

This article is a PNAS Direct Submission. J.T.R. is a guest editor invited by the Editorial Board.

[1]To whom correspondence should be addressed. E-mail: sarchibald@csir.co.za.

This article contains supporting information online at www.pnas.org/lookup/suppl/doi:10.1073/pnas.1211466110/-/DCSupplemental.

This approach ensures that we do not confound our response variable because we classify pyromes independently of vegetation and climate, allowing them to emerge from the multidimensional space occupied by the fire characteristics. Post hoc, we assess how closely associated biomes and pyromes are, and which climate and human variables drive variation in global fire regimes. The circumpolar boreal forest biome extends through North America and Russia, but fire regimes on the two continents differ: one is characterized by crown fires, and the other by surface fires (23). This suggests that a pyrome map of the world might look somewhat different from a biome map. In contrast, the probability of fire and the occurrence of the savanna biome coincide clearly across Africa, Australia, and South America (24).

Identification and Mapping of Key Fire Characteristics

Five important fire regime characteristics were identified and quantified globally at 0.5° resolution by using available remotely sensed data. These are fire return interval (FRI), maximum fire intensity, length of the fire season, maximum fire size, and mean annual area burned (Fig. S1 *A–E*), and they represent a significant advancement in the mining of satellite-derived information on fire—moving beyond indices of burned area to describe other ecologically meaningful metrics of fire (25) (*Materials and Methods*).

Fire intensity is a measure of the rate of energy released by fire, and FRIs are indicative of the growth period available to plants between fires. Changes in frequency or intensity of fires can alter vegetation community composition by promoting or excluding different types of plants (1, 2), and are important for feedbacks between vegetation and fire (26, 27). The size of individual fires and the length of the year over which fires occur reflect the continuity of the fuel bed and the propensity of the vegetation to be flammable (28, 29). Mean burned area is a widely used global measure of fire. It has been linked to the paleorecord (30), and is used to calculate fluxes of carbon from the biosphere to the atmosphere (3). Distinguishing fire type is important in assessing fire regimes, and we hoped that crown and ground fires would emerge as having distinctive combinations of fire characteristics.

Two of these datasets—fire size and FRI—have not been produced globally before. Previously published works (25, 31) and *SI Materials and Methods* detail their derivation and validation [the FRI metric is most reliable for return intervals less than 50 y (Fig. S2)].

Results and Discussion

Physical Limits of Fire. As expected, there was structure in multidimensional fire space and tradeoffs between particular fire characteristics. Fire intensity is strongly constrained where fires are frequent, but infrequent fires show a wide range of fire intensities (Fig. 1*A*). Ecologically, infrequent fire is associated with intense crown fire events and with low-intensity surface fires in tropical forests. When fire is frequent, there is insufficient time to accumulate the fuel needed for very high-intensity fires, and these systems are climatically too flammable to produce creeping, low-intensity fires.

Very long fire seasons are only associated with small fires (Fig. 1*B*). Long fire seasons are typical of human-derived management fires (28), which are also likely to be small (32), so this section of fire space might be a human creation.

Constraints between maximum fire size and area burned are not as tight as would be expected from studies that have found the majority of area to be burned in a few large fires (33). High burned areas can result from a range of fire size distributions (Fig. 1*C*). However, regions with very small fires do show slightly lower burned area. Finally, systems with short FRIs always show high area burned, but, at longer FRIs, the area burned ranges more widely (Fig. 1*D*). A complete set of bivariate relationships is shown in Fig. S3.

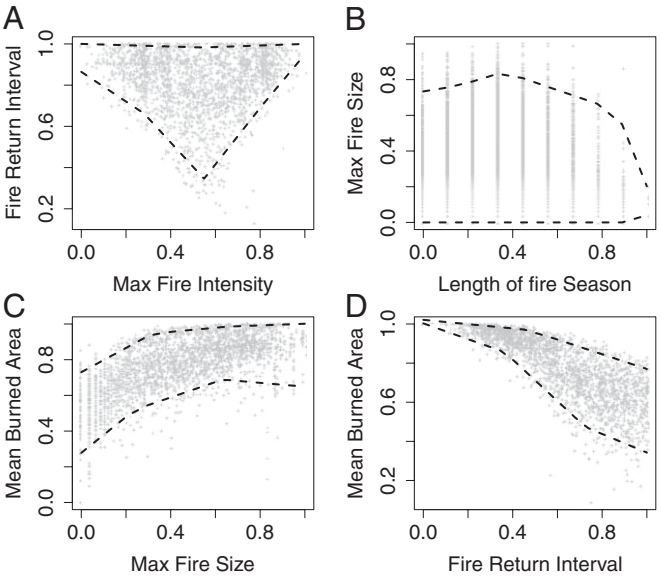

Fig. 1. Multidimensional fire space represented by selected combinations of fire characteristics. FRI by maximum fire intensity (*A*), fire season length by maximum fire size (*B*), maximum fire size by mean burned area (*C*), and FRI by mean burned area (*D*). For each combination there are constraints—presumably imposed through vegetation, climate, and people—which mean that not all of the space is occupied. Data are logged and rescaled. Dashed lines represent fifth and 95th piecewise quantile regression fits to the data. Fig. S3 shows graphs of all combinations.

These observed patterns challenge some of the prevailing assumptions around global fire relationships used to drive fire models and estimate fire emissions. Thonicke et al. (34) assume a correlation between fire season and area burned that is not apparent in our data, and Hao and Liu (35) overestimated emissions from Africa by assuming a log-linear relationship between FRI and area burned.

The results raise important questions about how amenable these patterns are to manipulation as a result of changes in climate or vegetation or by human management. It is possible that humans, by initiating burning of small agricultural fires at unpredictable times of year (28), pushed the system further into the lower right corner (i.e., small fires, long fire season) of Fig. 1*B* than it was before. Similarly, before C4 grasses evolved, very short annual and subannual FRIs (Fig. 1*A*) might not have existed on the globe.

Identifying Pyromes. We identified five distinct pyromes (*SI Materials and Methods*), each associated with particular combinations of fire characteristics (Fig. 2). Two of these pyromes have high annual burned areas and frequent fires (Table 1 and Fig. 3). These pyromes differ in their fire size and fire intensity, as well as their spatial distribution: Australia has larger, more intense fires [frequent–intense–large (FIL)], whereas in Africa, smaller, less intense fires dominate [frequent–cool–small (FCS)] (Fig. 2). Two more pyromes were identified with infrequent fires and very short fire seasons (Table 1 and Fig. 3). One has high-intensity, larger fires [rare–intense–large (RIL)], and the other has lower fire intensity and smaller fires [rare–cool–small (RCS)]. These pyromes dominate in temperate and boreal regions but occur elsewhere as well (Fig. 2).

A final pyrome was identified with intermediate fire return times but fairly small fires (Table 1 and Fig. 3). This intermediate–cool–small (ICS) pyrome occurs throughout the globe, particularly in regions of deforestation and agriculture (Fig. 2).

Table 1. Characteristics of the five pyromes identified by model-based expectation–maximization clustering

Characteristic	FIL (yellow)	FCS (orange)	RIL (green)	RCS (purple)	ICS (blue)
Mean burned area, %	14 (8–36)	9 (3–17)	1 (0–2)	0 (0–0.5)	0 (0–1)
Estimated FRI, y	3 (1–4)	1 (1–2)	>50	>50	12 (6–19)
Max FRP, MW	473 (350–660)	197 (156–253)	476 (283–844)	187 (108–334)	224 (143–352)
Max fire size, km^2	414 (155–1437)	25 (15–43)	83 (38–214)	4 (2–9)	9 (5–17)
Length of fire season, mo	4 (3–4)	3 (3–4)	2 (1–2)	1 (0–1)	3 (3–4)
Tropical moist broadleaf forests	2	10	5	**28**	**56**
Tropical dry broadleaf forests	3	21	6	16	**53**
Tropical coniferous forests	0	10	13	17	**59**
Temperate mixed forests	1	2	11	**41**	**45**
Temperate coniferous forests	2	0	**26**	**45**	**26**
Boreal forests	1	0	**46**	**47**	6
Tropical grasslands and shrublands	**29**	**33**	9	6	**23**
Temperate grasslands and shrublands	10	3	21	**29**	**37**
Flooded grasslands	**46**	17	8	5	**24**
Montane grasslands	6	15	13	**31**	**36**
Mediterranean vegetation	1	3	**25**	**36**	**35**
Xeric vegetation	18	1	**31**	**24**	**26**

The median and 25th to 75th quantiles of each fire characteristic are reported (parentheses), as are the percentages of 12 World Wildlife Fund biome classes that fall into each pyrome (values greater than 20% are bold, Table S1 shows for pyromes by biome).

The largest fires are found in the FIL pyrome (414 km^2 on average; Table 1), and the most intense fires are found in the RIL pyrome (476 MW). In FCS regions fires occur annually, whereas the RCS pyrome has an average FRI of more than 100 y. The shortest fire seasons are associated with RIL and RCS pyromes (less than 2 mo), and average area burned is hardly detectable in the RCS and ICS pyromes.

Correspondence of Pyromes to Biomes. Chuvieco et al. (9), by using three active fire data metrics, successfully distinguished boreal forest but found no clear patterns with other vegetation classes. In our study, more than 93% of the boreal forest falls into the RIL and RCS pyromes (green and purple, respectively) and we also found the FIL and FCS (yellow and orange, respectively) pyromes to be concentrated in tropical grasslands (Figs. 2–5). In contrast, xeric vegetation is associated with four of the five pyrome classes (Table 1), presumably depending on the type of fuels present in the particular arid system (shrubs, grasses, or tussock grasses).

Fires in tropical moist broadleaf forests are predominantly of the ICS (blue) type but this biome can also sustain RCS (purple) and FCS (orange) fires (Table 1). Almost all biomes contain a substantial proportion (>20%) of the ICS pyrome (Table 1). Our analysis did not distinguish between North American and Russian boreal fire regimes, although the fire intensity data showed the North American fires to be generally more intense (Fig. S1*C*).

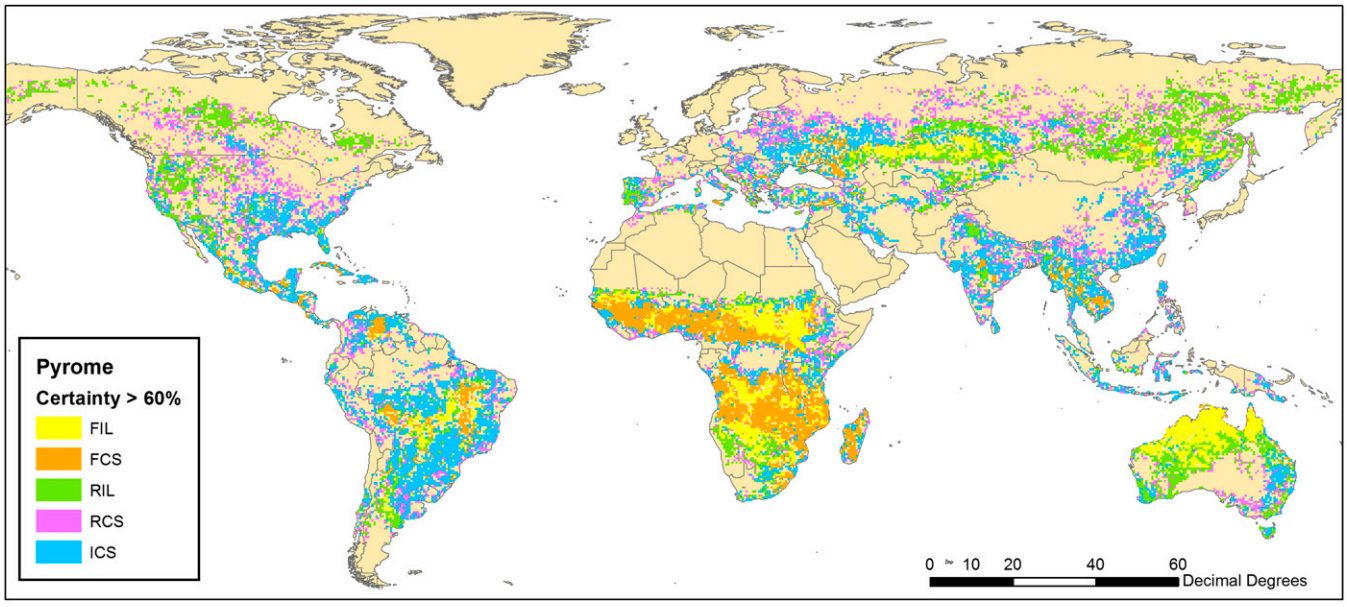

Fig. 2. Mapping the spatial distribution of pyromes. Produced from the five-cluster solution of a model-based expectation–maximization clustering algorithm. Pyromes represent regions of the globe that have similar fire frequencies, intensities, sizes, burned areas, and fire season lengths. Pixels with greater than 60% probability of being uniquely categorized are plotted (85% of the data).

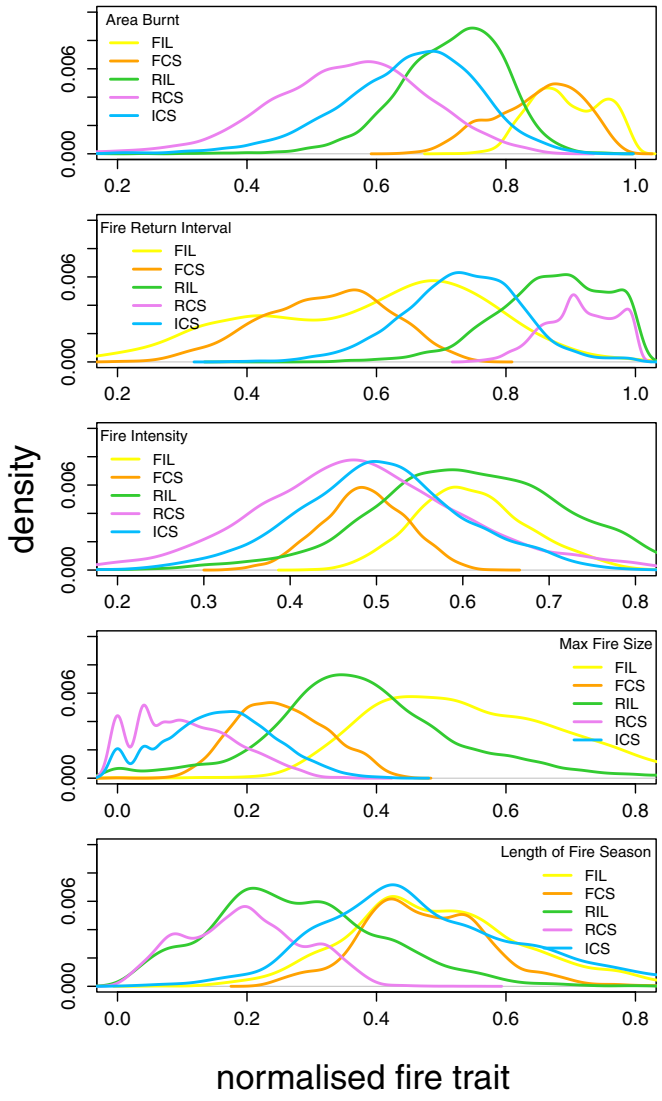

Fig. 3. Distinguishing pyromes using frequency distributions of fire characteristics. Data are logged and rescaled. Table 1 shows real values.

Environmental Correlates. Axes of mean annual temperature (MAT) and mean annual precipitation (MAP) have traditionally been used to describe the climatic determinants of biomes (18), but these metrics are not necessarily as strongly associated with pyromes. We identified three climate variables that would be expected to explain spatial variability in fire regimes: effective rainfall (i.e., productivity), interannual variability of rainfall (i.e., probability of long-term droughts affecting woody fuels), and seasonality of rainfall (i.e., probability of short-term droughts affecting grassy/litter fuels).

The five pyromes overlap substantially when plotted on axes of MAP and MAT (Fig. 4*A*), although it does appear that the two frequently burning pyromes (FIL and FCS) cover warmer, wetter climate space than the other pyromes. When plotted on axes that are more meaningful to fire, this inference is shown to be incorrect (Fig. 4*B*). Actually, frequently burning pyromes dominate in more arid ecosystems (measured by effective rainfall) than other pyromes. These pyromes are also associated with strong rainfall seasonality, which provides frequent (annual) opportunities for fire (Fig. 5).

Human impacts (HIs) on fire are globally apparent (30, 36). To examine this, we used an HI score that integrates information on human densities and land transformation (37). The HI score clearly distinguishes the ICS from the other pyromes. Crucially, we also found that pyromes characterized by large fires (FIL and RIL) are correlated with low HI (Fig. 5). These data suggest that human activities are a major force disrupting the fire system, and that human activities play an equal role to climate in determining current pyromes. For example, the difference between the two grassy fire regimes (FIL and FCS) is most clearly explained by their differences in HI than by any climatic drivers, and they probably represent a "sparsely habited grassy pyrome" and a "densely habited grassy pyrome," respectively.

Relation of Pyromes to Known Fire Regimes. Despite the absence of clear correspondence among climate, biomes, and pyromes, a basic dichotomy between the pairs of frequently burnt vs. infrequently burnt pyromes can be distinguished (Fig. 3). This dichotomy probably reflects a division between ecosystems dominated by alternative fuel types (grasses vs. litter).

Only grasses have the physiological capacity to regrow lost biomass quickly enough to sustain the frequent (i.e., every 1–3 y) fire regimes characteristic of the FIL and FCS pyromes. This is corroborated by their dominance in regions of tropical and temperate grassland (Fig. 2), and their association with high rainfall seasonality—a climatic characteristic of C4 grassy ecosystems (38). Respectively, 91% and 68% of these two pyromes are classified as grassland vegetation of some sort.

Only the RIL pyrome has the combined high fireline intensity (close to 500 MW) and long fire return times (>30 y) that would be associated with crown fires. This pyrome prevails in broadleaf and needleleaf forests, is found wherever there is Mediterranean vegetation (Iberian peninsula, west coast of the United States, southwestern Australia), and also in the spinifex grasslands of Australia (Fig. 2). It is often interspersed geographically with the RCS pyrome—presumably, surface fires burning through litter fuels in the same vegetation.

Reported FRIs for crown fire regimes range from approximately 15 y in fynbos (39) to approximately 150 y in conifer forests (40). Our data were unable to distinguish these and only identified one crown fire pyrome. With better global FRI data, more subtle distinctions in crown fires might become apparent. It appears, however, that the distinction between different types of crown fires is small relative to global variation in fire characteristics, and that there is convergence in the fuel characteristics, if not the vegetation characteristics of these divergent ecosystems.

The prevalence and ubiquity of the ICS pyrome suggest that this is a human-derived pyrome (41). It is characterized by very small fires (ranging from 5 to 17 km^2), which are a known consequence of human landscape transformation that creates physical barriers to fire spread (25, 32). In other characteristics, this pyrome represents a homogenization of the extreme characteristics of other pyromes (Fig. 3), and it cuts across vegetation types from tropical broadleafed forests to xeric vegetation (Table 1). This would be expected of a fire regime consisting of fires lit by people for specific purposes, and therefore less closely connected to vegetation and climate drivers.

Implications. These data and several recent papers (42, 43) support our contention that fire is unlikely to be unilaterally responsive to climate in a deterministic way. The pyromes characteristic of the modern world can be explained with reference to current vegetation and climate, but complex interactions among fire, climate, vegetation, and modern human activities impede our ability to predict emergent fire regimes.

Whitlock et al. (6), in recognizing these vegetation–fire–climate contingencies, suggest that a fire regime be defined as "the full range of variability in fire activity within a given vegetation type." Our analysis shows that pyromes are not simply a construct of biomes. One biome can contain different fire regimes, and con-

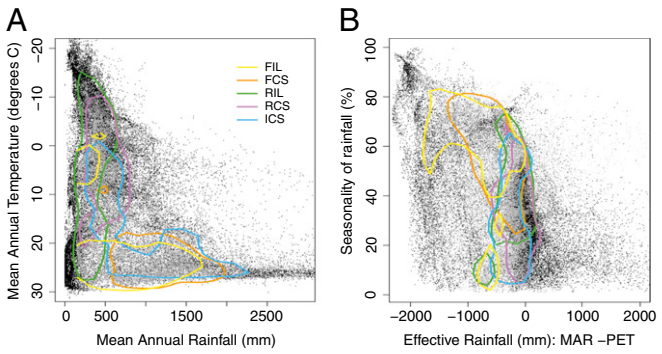

Fig. 4. Plotting pyromes in climate space. A Whittaker plot (MAP–MAT) does not clearly distinguish pyromes as it does with vegetation (*A*). Meaningful climate indices improve the separation (*B*), but pyromes are not determined by climate alone. Black points show all vegetated 0.5° grid cells, gray points show all cells that had fire data. Lines show the 95th quantile of the density of points for each pyrome class.

trasting biomes, such as xeric shrublands and boreal forests, may effectively converge on a common pyrome through similarity in the underlying dominant fuel type and growth constraints on fuel development.

There do appear to be predictable relationships between fuel types and fire characteristics, so developing spatial data on fuel characteristics (e.g., flammability of fuels, litter structure, propensity for crown fire) might help to clarify the links between vegetation and fire. Similarly, choosing meaningful climate indices that relate directly to how climate controls the amount and type of fuel and its propensity to be flammable would undoubtedly make climate–fire relationships clearer.

This spatial analysis corroborates meta-analyses of charcoal records, which suggest that HIs have acted to decouple the fire–climate signal in recent years (44). The current spatial extent of the human-modified pyrome (Fig. 2), and the superior predictive power of our HI score over climate indices (Fig. 5), point to the significant role humans can play in determining fire characteristics and driving future fire regimes.

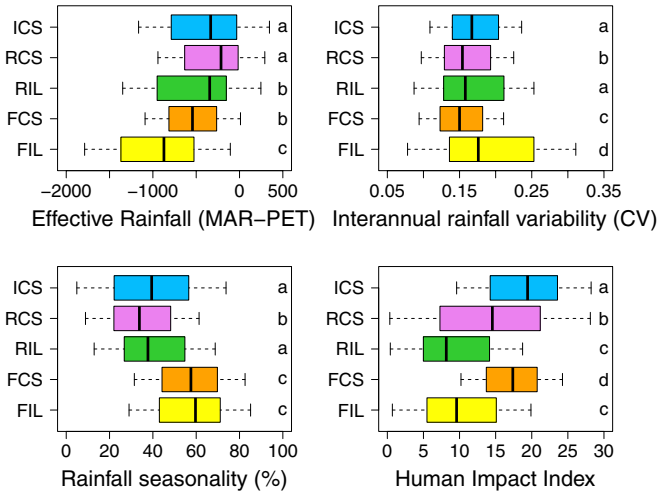

Fig. 5. Environmental characteristics of the five pyromes. The climate variables were chosen to represent important drivers of fire (see text and *SI Materials and Methods*). Lines represent the median, boxes the 25th and 75th quantiles, and whiskers the 0.5× interquartile range of the data. Significantly different distributions (two-sided *t* test) are indicated with letters.

The pyromes described here depend on the fire characteristics included, on the number of clusters chosen, and on the limitations of data used to represent each fire characteristic (*SI Materials and Methods*), and are unlikely to be definitive. Moreover, the 14-y data record effectively sets the time period over which we are describing global fire regimes, and is only a snapshot of a continuously changing system. However, the spatially explicit nature of our data and the range of fire metrics used complements longer-term, less data-rich studies (see ref. 45 for justification). Our pyromes could be useful to global fire modelers as a test of their ability to replicate the different types of fires apparent on the globe today. Moreover, the use of pyromes as well as biomes as categories to estimate emissions from wildfires could constrain some of the uncertainty—for example, by providing meaningful fire units for Intergovernmental Panel on Climate Change (IPCC) look-up tables.

Ultimately, we require confidence in our ability to infer past pyromes, and to predict patterns of world fire we might experience in the future. It is clear from this analysis that not all combinations of fire characteristics are possible (Fig. 1), and that various factors constrain modern fire regimes. These constraints appear to be defined by energetics: interactions between fuel type, climate, atmospheric chemistry, and rates of regrowth after fire (13). It is also clear that HIs, novel climates, and evolving vegetation can alter the type of fire that occurs in a location (15, 17, 27, 46–48). Whether these impacts are shifting the occurrence of fire within the multidimensional fire space identified here (Fig. 1), or releasing some of the important constraints on fire and allowing fire regimes to move into novel parts of this space is not yet clear.

Materials and Methods

Data Preparation. The datasets were produced using global remotely sensed estimates of active fire and burned area [moderate-resolution imaging spectroradiometer (MODIS) MCD45A1, MCS14ML, and Global Fire Emissions Database (GFED) 3.1]. These are available for a minimum of 10 y (operational MODIS sensors; however, the GFED3 burned area product provides a 14-y time series) and a minimum of 500 m spatial resolution. The short observational time period is an obvious constraint to characterizing fire regimes in systems which burn infrequently, but we chose indices that maximized the information that could be gained from these global datasets (*SI Materials and Methods*). The analysis was run for all 0.5° grid cells in which there was fire information (26,455 data points).

We summed the 0.5° GFED3.1 monthly burned area data to produce an annual measure of area burned from 1997 to 2010 and averaged this produce mean area burned (Fig. S1*A*). Satellite middle-IR wavelength measurements sensed over actively burning fires can quantify the rate of radiant energy release: the fire radiative power (FRP) (49). We used the MCD14ML active fire product to calculate the 95th quantile of FRP as a proxy for the maximum fireline intensity (Fig. S1*B*). FRI is usually estimated by fitting a Weibull distribution to fire return time data (50). This method resulted in convergence of FRI estimates for only some portions of our global FRI dataset (*SI Materials and Methods*). The coefficient of variation (mean/SD) in annual burned area (CVBA) correlates well with FRI ($R^2 = 0.67$; Fig. S2) because interannual variability in area burned is higher when fires occur infrequently. We calculated CVBA from the GFED3.1 data product (Fig. S1*C*). Individual fires can be identified from burned area data by using a flood-fill algorithm (31). We did this for the globe by using the MCD45A1 burned area product (*SI Materials and Methods*) and used the 95th quantile of fire size in each grid cell to give maximum fire size (Fig. S1*D*). The length of the fire season was quantified as the number of months required to reach 80% of the total average annual burned area (Fig. S1*E*).

Climate characteristics were quantified from the 0.5° Climatic Research Unit (University of East Anglia) long-term global climate data (www.cru.uea.ac.uk/; accessed November 2011) and the WorldClim dataset (www.worldclim.org; accessed November 2011). The difference between MAP and mean annual potential evapotranspiration (i.e., effective rainfall) produces an index of productivity whereby anything less than zero indicates that evaporative demand exceeds incoming precipitation. We used a rainfall concentration index (51) to describe rainfall seasonality. Longer-term wetting and drying events can also impact the probability of fire (47), and to represent this we used the coefficient of variation in annual rainfall. We used the HI index (37) to

represent the effects of people on ignitions and land connectivity. We used the WWF terrestrial ecoregions map, which is the only global product derived from ground-truthed vegetation maps, and which identifies 14 different global biomes. Although it uses climate qualifiers to classify biomes, which is something we were aiming to avoid in our pyromes classification, it gives a better description of the fuels than other modeled or remotely sensed biome products (*SI Materials and Methods*).

Analysis. Except where indicated, the nonnormal data (FRI, maximum FRP, CVBA, maximum fire size, mean burned area) were logged, and all data were rescaled between 0 and 1 and centered. A principal components analysis was run using the princomp package in the open-source R statistical software. All five fire characteristics contributed significantly to the principal components and were largely orthogonal to each other (Fig. S4). Constraints and tradeoffs between different fire characteristics were demonstrated by plotting each characteristic against the others, by using a piecewise quantile linear regression (and the R statistical package quantreg) to identify the fifth and 95th quantiles of the data. The Mclust package was used to identify regions of similar fire regimes (pyromes). This package allows statistical comparison of different cluster sizes and the shapes of the clusters using the Bayesian information criterion (BIC). Importantly, it also allows for estimation of uncertainty around classifications by using expectation maximization methods (52), and for predicting the grouping of points not used in the original analysis based on their attributes. We used a default prior with two clusters and a variable shape, variable volume, variable orientation (VVV) model to regularize the fit to the data. An initial analysis using all possible parameterizations of the covariance matrix and cluster sizes from two to 15 indicated that a VVV model gave the best results (i.e., highest BIC). Choosing the correct number of clusters (i.e., pyromes) was difficult because the BIC continued to increase to 15 clusters. Beyond five clusters, the increase in BIC was negligible (Fig. S5) and did not justify further splitting of the data. As a result of processor constraints, we ran Mclust on a training sample of 10,900 points and predicted the pyrome of the remaining approximately 15,000 points by using discriminant analysis (mclustDAtrain and mclustDAtest). All points were classified into one of five pyromes with an associated uncertainty value. Uncertainties were fairly constant across pyromes, with most points having uncertainty values less than 0.2 and no clear spatial pattern emerging (Fig. S6). Fig. S7 indicates how the five pyromes emerged from the clustering procedure.

ACKNOWLEDGMENTS. The authors thank William Bond for his helpful comments on an earlier draft and two anonymous reviewers who instilled more rigor in our FRI analysis. This work was supported by Mark Westoby, and funded by the Australian Research Council–New Zealand Vegetation Function Network and the Council for Scientific and Industrial Research Young Researchers' Establishment Fund (S.A.).

1. Gill AM (1975) Fire and the Australian flora: A review. *Aust For* 38:4–25.
2. Bond WJ, Keeley JE (2005) Fire as a global 'herbivore': The ecology and evolution of flammable ecosystems. *Trends Ecol Evol* 20(7):387–394.
3. van der Werf G, et al. (2010) Global fire emissions and the contribution of deforestation, savanna, forest, agricultural, and peat fires (1997–2009). *Atmos Chem Phys Discuss* 10:16153–16230.
4. Moritz MA (2003) Spatiotemporal analysis of controls on shrubland fire regimes: Age dependency and fire hazard. *Ecology* 84:351–361.
5. Keeley JE, Fotheringham CJ, Morais M (1999) Reexamining fire suppression impacts on brushland fire regimes. *Science* 284(5421):1829–1832.
6. Whitlock C, Higuera P, McWethy D, Briles C (2010) Paleoecological perspectives on fire ecology: Revisiting the fire-regime concept. *Open Ecology Journal* 3:6–23.
7. Dwyer E, Pinnock S, Gregoire J, Pereira J (2000) Global spatial and temporal distribution of vegetation fire as determined from satellite observations. *Int J Remote Sens* 21:1289–1302.
8. Giglio L, van der Werf G, Randerson J, Collatz G, Kasibhatla P (2006) Global estimation of burned area using MODIS active fire observations. *Atmos Chem Phys* 6:957–974.
9. Chuvieco E, Giglio L, Justice C (2008) Global characterization of fire activity: Toward defining fire regimes from earth observation data. *Glob Change Biol* 14:1488–1502.
10. Meyn A, White P, Buhk C, Jentsch A (2007) Environmental drivers of large, infrequent wildfires: The emerging conceptual model. *Prog Phys Geogr* 31:287–312.
11. Bradstock RA (2010) A biogeographic model of fire regimes in Australia: Contemporary and future implications. *Glob Ecol Biogeogr* 19:145–158.
12. Krawchuk MA, Moritz MA (2011) Constraints on global fire activity vary across a resource gradient. *Ecology* 92(1):121–132.
13. McKenzie D, Miller C, Falk D, eds (2011) *The Landscape Ecology of Fire* (Springer, New York).
14. Wright IJ, et al. (2004) The worldwide leaf economics spectrum. *Nature* 428(6985):821–827.
15. D'Antonio C, Vitousek P (1992) Biological invasions by exotic grasses, the grass/fire cycle, and global change. *Annu Rev Ecol Syst* 23:63–87.
16. Syphard AD, Radeloff VC, Hawbaker TJ, Stewart SI (2009) Conservation threats due to human-caused increases in fire frequency in Mediterranean-climate ecosystems. *Conserv Biol* 23(3):758–769.
17. Westerling AL, Hidalgo HG, Cayan DR, Swetnam TW (2006) Warming and earlier spring increase western U.S. forest wildfire activity. *Science* 313(5789):940–943.
18. Whittaker R (1975) *Communities and Ecosystems* (MacMillan, New York), 2nd Ed.
19. Bond WJ, Woodward FI, Midgley GF (2005) The global distribution of ecosystems in a world without fire. *New Phytol* 165(2):525–537.
20. Beerling D (2008) *The Emerald Planet. How Plants Changed Earth's History* (Oxford Univ Press, Oxford), Vol 145.
21. Wang Z, Chappellaz J, Park K, Mak JE (2010) Large variations in Southern Hemisphere biomass burning during the last 650 years. *Science* 330(6011):1663–1666.
22. Westoby M (1998) A leaf-height-seed (lhs) plant ecology strategy scheme. *Plant Soil* 199:213–227.
23. Wooster M, Zhang Y (2004) Boreal forest fires burn less intensely in Russia than in North America. *Geophys Res Lett* 31:L20505.
24. Lehmann CE, Archibald SA, Hoffmann WA, Bond WJ (2011) Deciphering the distribution of the savanna biome. *New Phytol* 191(1):197–209.
25. Archibald S, Scholes R, Roy D, Roberts G, Boschetti L (2010) Southern African fire regimes as revealed by remote sensing. *Int J Wildland Fire* 19:861–878.
26. Hoffmann WA, Solbrig OT (2003) The role of topkill in the differential response of savanna woody species to fire. *For Ecol Manage* 180:273–286.
27. Brubaker LB, et al. (2009) Linking sediment-charcoal records and ecological modeling to understand causes of fire-regime change in boreal forests. *Ecology* 90(7):1788–1801.
28. Le Page Y, Oom D, Silva J, Jönsson P, Pereira J (2010) Seasonality of vegetation fires as modified by human action: observing the deviation from eco-climatic fire regimes. *Glob Ecol Biogeogr* 19:575–588.
29. Miller C, Urban D (2000) Connectivity of forest fuels and surface fire regimes. *Landscape Ecol* 15:145–154.
30. Bowman DMJS, et al. (2009) Fire in the Earth system. *Science* 324(5926):481–484.
31. Archibald S, Roy D (2009) Identifying individual fires from satellite-derived burned area data. *Proc IGARSS* 3:160–163.
32. Niklasson M, Granstrom A (2000) Numbers and sizes of fires: Long-term spatially explicit fire history in a Swedish boreal landscape. *Ecology* 81:1484–1499.
33. Strauss D, Bednar L, Mees R (1989) Do one percent of forest fires cause ninety-nine percent of the damage? *For Sci* 35:319–328.
34. Thonicke K, Venevsky S, Sitch S, Cramer W (2001) The role of fire disturbance for global vegetation dynamics: Coupling fire into a Dynamic Global Vegetation Model. *Glob Ecol Biogeogr* 10:661–677.
35. Hao WM, Liu MH (1994) Spatial and temporal distribution of tropical biomass burning. *Global Biogeochem Cycles* 8:495–503.
36. Aldersley A, Murray SJ, Cornell SE (2011) Global and regional analysis of climate and human drivers of wildfire. *Sci Total Environ* 409(18):3472–3481.
37. Sanderson E, et al. (2002) The human footprint and the last of the wild. *Bioscience* 52:891–904.
38. Keeley JE, Rundel PW (2005) Fire and the Miocene expansion of C4 grasslands. *Ecol Lett* 8:683–690.
39. Van Wilgen BW, et al. (2010) Fire management in Mediterranean-climate shrublands: A case study from the Cape fynbos, South Africa. *J Appl Ecol* 47:631–638.
40. Carcaillet C, et al. (2001) Change of fire frequency in the eastern Canadian boreal forests during the Holocene: Does vegetation composition or climate trigger the fire regime? *J Ecol* 89:930–946.
41. Bowman DM, et al. (2011) The human dimension of fire regimes on Earth. *J Biogeogr* 38(12):2223–2236.
42. Staver AC, Archibald S, Levin SA (2011) The global extent and determinants of savanna and forest as alternative biome states. *Science* 334(6053):230–232.
43. Shugart H, Woodward F (2011) *Global Change and the Terrestrial Biosphere: Achievements and Challenges* (Wiley-Blackwell, New York).
44. Marlon J, et al. (2008) Climate and human influences on global biomass burning over the past two millennia. *Nat Geosci* 1:697–702.
45. Daniau AL, Bartlein PJ, Harrison SP, et al. (2012) Predictability of biomass burning in response to climate changes. *Glob Biogeochem Cycles* 26:GB4007.
46. Flannigan MD, Krawchuk MA, de Groot WJ, Wotton BM, Gowman LM (2009) Implications of changing climate for global wildland fire. *Int J Wildland Fire* 18:483–507.
47. Swetnam TW, Betancourt JL (1990) Fire-southern oscillation relations in the southwestern United States. *Science* 249(4972):1017–1020.
48. Russell-Smith J, et al. (2003) Contemporary fire regimes of northern Australia, 1997-2001: Change since aboriginal occupancy, challenges for sustainable management. *Int J Wildland Fire* 12:283–297.
49. Kaufman Y, et al. (1996) Relationship between remotely sensed fire intensity and rate of emission of smoke: SCAR-C experiment. *Global Biomass Burning*, ed Levine J (MIT Press, Cambridge, MA), pp 685–696.
50. Johnson E, Gutsell S (1994) Fire frequency models, methods and interpretations. *Adv Ecol Res* 25:239–287.
51. Markham C (1970) Seasonality of precipitation in the United States. *Ann Assoc Am Geogr* 60:593–597.
52. Fraley C, Raftery A (2007) Bayesian regularization for normal mixture estimation and model-based clustering. *J Classification* 24:155–181.

Supporting Information

Archibald et al. 10.1073/pnas.1211466110

SI Materials and Methods

Identifying and Extracting Metrics of Fire Characteristics from Global Remotely Sensed Data. All five fire characteristics used in the analysis could be quantified by using global remotely sensed fire datasets.

Average area burned. Mean burnt area is currently the most commonly investigated aspect of global fire. It can easily be linked with data from the paleorecord and global vegetation models and is necessary for calculating emissions and fluxes from the biosphere to the atmosphere. In uniform landscapes, mean burned area can be representative of the fire return time, but our analysis shows that the two indices actually represent different aspects of fire, and that there are parts of the world with low burned areas that burn very frequently.

Because burned area is used for so many applications, there are several global datasets available. We summed the 0.5° Global Fire Emissions Database (GFED) 3.1 monthly burned area data (1) to produce an annual measure of area burned from 1997 to 2010 and averaged this over the 14-y dataset (Fig. S1*A*).

Fire intensity. Fireline intensity is a measure of the rate of energy released from a fire per unit length of the burning front. It has traditionally been calculated as the product of the dry weight of biomass burned, the energy content of the fuel, and the rate of spread of the fire (2). Fire intensity measures are likely to help distinguish between ground fire and crown fire regimes—the former burning at lower intensities because they are burning less fuel and spreading slowly. Fires with higher fireline intensities might also be spreading rapidly, burn for longer, and burn larger parts of the landscape—they are less likely to be extinguished by nighttime weather conditions, moist fuels, or topographic barriers. Ecologically, fireline intensity is related to flame length and has effects on the size class of trees that are top-killed and on the patchiness of a burn (but see ref. 3 for a discussion of the limitations of using fire intensity as an index of ecosystem response to fire).

Satellite middle-IR wavelength measurements sensed over actively burning fires can be used to calculate the rate of radiant energy release: the fire radiative power (FRP) (4). This is measured in units of megawatts per pixel. So far, it has largely been used to quantify the amount of biomass burned by fires in Africa (5, 6). It could also be used as a spatially and temporally continuous measure of the fireline intensity (7)—one that can be quantified globally at 0.5° resolution.

The energy released by individual fires varies greatly over the duration of the fire: for example, grassland fire FRP has been observed to change by an order of magnitude with the wind direction relative to the unburned fuel bed (7), and, at night, the fire intensity is typically much lower. For this reason, most FRP datasets are heavily skewed toward very low values. We tried several metrics of fireline intensity—median, maximum, and range of FRP values in a 0.5° grid cell. The best information was provided by the 95th quantile, which distinguishes systems that have the potential to burn at very high intensities (crown fires) from those in which there is insufficient fuel to result in high-intensity fires. Using the 95th quantile instead of the maximum avoids errors caused by outliers and wrong values (8). At present, this index cannot be directly related to the conventional measure of fireline intensity (kW/m) because the length of the flame front is not known. There is ambiguity because a very small, very intense fire could have the same FRP value as a very large, less intense fire.

FRP values from the moderate-resolution imaging spectroradiometer (MODIS) global monthly fire location product (MCD14ML) were used to calculate the fire intensity index. The native resolution of these products is 1 km, so the FRP values are in units of megawatts per 1-km pixel. All active fire points over all years in each 0.5° grid cell were used, and the 95th quantile of this distribution was extracted and mapped (Fig. S1*B*). The 95th quantile correlates very strongly with the range of FRP values, as well as the median FRP value.

Fire return time. Return times are indicative of the intervening growth period available to plants between fires. Observed fire return intervals (FRIs) range from years to decades to thousands of years based on data from lake records, tree rings, ocean cores, and the reproductive and life history traits of the vegetation. Areas with short fire return times tend to be dominated by resprouting woody species and/or grasses. Areas characterized by long fire return times tend to be dominated by obligate seeding woody species. A circularity arises, however, as resprouters and grasses can recover flammable biomass more quickly than reseeding species, so it is often not clear whether the vegetation is driving the fire return time or the fire return time is driving the vegetation. Investigation of global patterns of fire return time in relation to climate and vegetation might help us to better understand these feedbacks and constraints.

However, fire return time is one of the most difficult fire regime measures to acquire, even for single locations, and, because of the different time scales involved and the idiosyncrasies of different fire history datasets, it is difficult to assemble anything coherent at global scales. It is common to use the average area burned as an estimate of FRI. The reciprocal of area burned gives the estimated fire return time in years (i.e., if one fourth of the landscape burns on average, the estimated return time for fire is 4 y). This "space-for-time" substitution breaks down if some parts of the landscape burn very often and other parts of the landscape hardly burn at all (discussed in ref. 9).

The standard approach to estimating fire return periods involves fitting a distribution (usually the Weibull distribution) to a set of individual fire interval records, and accounting for the censoring that occurs at the beginning and end of the record period (10–12). This method is well developed but it requires long datasets with enough interfire intervals to develop a reasonable distribution of intervals. The larger the FRIs, the longer the datasets required to get reasonable distributions. Although more robust to variable landscapes than space-for-time substitution, these methods also make the assumption that the landscape being considered comes from one distribution (i.e., has a uniform fire regime) (10), and would also become unreliable if different parts of the landscape burn at different frequencies. We used fire interval data from the 10-y MODIS fire datasets to fit Weibull distributions to 0.5° gridded data for the globe by using exactly the same methods as Archibald et al. (9), but the results often did not converge, or returned invalid FRI values, as the data were prone to the aforementioned problems of short time scales and nonuniform landscapes within the 0.5° grid. It could therefore not be used in the main analysis.

One alternative measure that, as far as we know, has never been investigated is to use information on the coefficient of variation (CV) of annual burned area as an index of fire return times. Areas that burn often should have a lower CV of burned area than areas that burn infrequently because the interannual variability in area burned would be higher when fires occur infrequently. This measure makes use of spatial and temporal data, and might

therefore be the most robust option for global remotely sensed datasets, which have short record periods (10–14 y) but high spatial coverage. We used the mean and SD of the 0.5° 14 y GFED3 burned area record to generate a CV of annual burned area to produce our index of fire return time.

To test this, we acquired four different FRI datasets—one from Africa from a published dataset on fire regimes across a range of different vegetation types and human land use intensities (9), one from the United States from a published dataset of FRIs (13), and two from long-term fire datasets from Australia (in Arnhem Land in the Northern Territory, and for the entire state of New South Wales in the southeast). This gave us 245 FRI records ranging from 1 y to 200 y in a variety of vegetation types for validation. A linear model fit to these data had an R^2 of 0.60 (Fig. S2). As suspected, there is some saturation of our CV in annual burned area (CVBA) index (probably because the short time period of the MODIS data), and values of CVBA greater than 3.4 represent a wide range of FRIs. Because of this we also tried fitting a logistic function, which improved the fit ($R^2 = 0.67$) but did not substantially reduce the model error (it reduced the rms error from 3 to 2.4). From Fig. S2, it is clear that our index can resolve FRIs less than 50 y and that we can identify regions with FRIs greater than 50 y, but our index is inadequate for accurately predicting these long FRIs. However, this still represents a vast improvement over the 10-y satellite data product. Further, as the duration of the satellite dataset extends, our index will become exponentially better at predicting the longer FRIs. We have used the logistic fit in our reported results (Table 1 and Fig. S1*C*).

Fire size. Fire size is an important attribute that defines fire activity. Intense fires are more likely to propagate rapidly, so some relationship between fire size and fire intensity is expected. We can also expect some inverse relationship between fire size and length of the fire season: if all available fuel is combusted in one large fire, the length of the fire season will be limited. The topology of the landscape, through the existence of patches of land that cannot carry fires, and which therefore act as blocks to the spread of fires, will also have an impact on fire size. In relation to this last point, the FRI might also have an impact on fire size by bisecting the landscape further by presenting recent burn scars as barriers to fires. There is plenty of literature available in this subject: Malamud et al. (14) show that fire size can be modeled by using a heavy-tailed distribution (i.e., a power law), indicating that most fires are small, with a few rare large fires responsible for a large proportion of the total burned area (15).

Spatial information on fire spread and fire size distributions is very rare, and, like fire return time, available only at few locations at which detailed records of individual fire scars have been kept. Previously, we developed a method for identifying individual fires from the MODIS burned area dataset by using a flood-fill algorithm, which assumes that pixels that are adjacent to each other and burn within a short enough time period have burned in the same fire (16). This has been used successfully to explore fire size distributions and the effect of humans on fire size and fire number in Africa (9).

For this analysis, we applied this approach to the global MCD45A1 MODIS burned area product (17). A pixel that is adjacent to another pixel (assuming an eight-pixel neighborhood) is assumed to belong to the same burn scar if the reported dates of burn are within 2 d of each other. Pixels that were flagged as fires detected with contextual decision rules (i.e., quality flag values of three or four) were excluded. In some areas, slightly more complicated segmentation algorithms were tested, but the results were not significantly different to those obtained with the use of a simple region-growing algorithm.

The chosen approach is simple and effective to implement on a global scale from the MODIS burned area product, but it has some shortcomings that ought to be mentioned. In brief, the assumptions are that the omission and commission errors are small, and that the timing of the detection can be used to minimize inappropriate merging of individual burn scars through commission errors. In general, errors of omission are more prevalent than errors of commission, and this translates to a more fragmented fire size distribution, with large fires being split into smaller fires. This effect is somehow counteracted by individual patches being incorrectly merged together as a result of individual fires occurring in adjacent pixels within the 2-d difference period. The reported minimum accuracy of the date of burn of the MCD45A1 product is 8 d, but we chose the 2-d threshold by testing these dates against the dates of MODIS active fire hotspots.

This fire size dataset has been tested against field data on fire perimeter in Africa (16) and in the Western United States (18), and validation is in progress in a number of different ecosystems globally. As with FRP, distributions of fire sizes are heavily skewed toward small numbers (in all landscapes, there are very few large fires relative to small fires). The 95th quantile of fire size in each 0.5° grid cell (Fig. S1*D*) was therefore similarly used as our global index of fire size to distinguish between landscapes where fires can spread and ones where maximum fire area is constrained.

Length of fire season. It would be expected that the temporal patterns of fire would give information to distinguish different types of fire regimes. Systems in which weather conditions are rarely suitable for burning would likely have shorter, more punctated bursts of fire, compared with seasonally dry tropics, which can be flammable for more than half the year. People have also been shown to interfere with annual cycles of flammability—anticipating as well as extending the fire season beyond that which is predicted from weather (19).

To represent these differences in fire regime, we chose to use an index of the length of the fire season. This was also calculated by using the GFED3 burned area product. First, a monthly climatology of burned area was produced from the entire time series. The monthly burned areas were then ranked, and the average fire season length was defined as the number of months required to reach 80% of the total average annual burned area (Fig. S1*E*) (analysis of values from 70% to 85% showed that the results were not sensitive to the threshold chosen). This index has been used successfully to define seasonal patterns of rainfall (20). Its advantages are that it is totally independent of area burned and makes no assumptions about the seasonal pattern of burning—for example, it can accommodate bimodal fire patterns (two fire seasons in 1 y). Although it is a continuous rather than a categorical variable, it consists of integer values ranging from 1 to 9 mo globally, which became problematic in clustering methods when the number of clusters approached nine. As the most appropriate cluster size emerged at five clusters, this was not problematic.

Alternative seasonality measures include the CV of monthly burned area (not a bounded measure; can be skewed by very low or very high annual burned area values), or a modification of the rainfall concentration index (21), which uses vector algebra to indicate how concentrated fires are in the year but is not reliable in bimodal systems.

Identifying and Extracting Climatic, Vegetation, and Human Variables from Global Remotely Sensed Data. At its simplest, the occurrence of fire is driven by the availability of fuels, and the flammability of these fuels—i.e., the amount of biomass, the moisture content of the biomass, and the prevailing weather conditions (22, 23). We identified three indices that could represent these factors globally to explore how well climate variables could distinguish the five pyromes. The 0.5° Climatic Research Unit (University of East Anglia) long-term global climate data (www.cru.uea.ac.uk/; accessed November 2011) were used for all rainfall calculations, and mean annual potential evapotranspiration was obtained

from the WorldClim dataset (www.worldclim.org; accessed November 2011) and averaged to 0.5° resolution.

Effective rainfall. The amount of biomass is largely controlled by the productivity of the system. Globally productivity is strongly related to available moisture, which in turn is related to rainfall and the evaporative demand of the system. Various measures of plant-available moisture exist (24), and we chose to use the difference between mean annual precipitation and mean annual potential evapotranspiration, which gives a value ranging from approximately −2,000 mm to 2,000 mm, wherein anything less than zero represents an environment in which evaporative demand exceeds incoming precipitation.

Seasonality of rainfall. In systems that experience regular drying and wetting periods, the availability of flammable conditions is much higher, and one would expect this to have an impact on the frequency, the intensity, the seasonality, and the size of fires, as well as the total area burned. Rainfall is distributed differently within the year across the globe, and some regions have much more seasonal rainfall, and more extended periods of flammability. We represented this by using a rainfall concentration index (21), which assesses the degree to which rainfall is equally dispersed over a 12-mo period. The index ranges from 0 (i.e., all months contribute equally to total annual rainfall) to 100 (i.e., all rainfall fell in 1 mo) and is entirely independent of the total amount of rainfall that falls in a year.

Interannual variability of rainfall. Periods of wetting and drying can occur over time scales longer than 1 y, and many parts of the world experience periodic multiannual droughts or several years of above-average rainfall. These longer-term wetting and drying events can also impact the probability of fire (25–27), and, to represent this, we used the CV (mean/SD) in annual rainfall.

Human impact index. The effects of humans on fire regimes has been explored by using indices such as population density, Gross Domestic Product, percentage of transformed land, and road density (20, 28, 29). The human impact index (30) is a global product that integrates information on all of these factors to product a score from 0 to 100 representing how impacted a landscape is by human activities. We used this as a single index that would represent the multiple effects of people on ignitions and on land connectivity, and took the median value per 0.5° grid cell.

Vegetation data. Ideally, we would have wanted to define important vegetation indices in the same way that we identified and extracted climate indices, and to explore how fire characteristics are dispersed in vegetation trait space. Unfortunately, theory and data on this are not well developed. We suspect that these vegetation indices would relate to the flammability of the fuels (specific leaf area, phosphorus content), the 3D packing of the fuels, and the propensity for crown fires.

It was possible, however, to explore how pyromes related to biomes, and whether there were unique pyromes associated with specific biomes. We used the World Wildlife Fund terrestrial ecoregions map, which identifies 14 different global biomes. This is the best available global vegetation map for our purposes, as it is derived from a compilation of ground-truthed vegetation maps rather than being a modeled product or derived from remotely sensed data. Biome maps derived from dynamic global vegetation models still do a very poor job of predicting the distribution of vegetation across the tropics, in particular, the distribution of savanna vs. forest. Given that the vast majority of the world's fire is contained within savannas, it would be inappropriate to use vegetation maps derived from model predictions. Maps derived from remote sensing usually use tree cover or leaf area index, and, although they can categorize vegetation structure, they are often inadequate for identifying biomes. Different biomes can have a similar level and ranges of woody cover but be functionally distinct, occupied by plant functional types that have vastly different effects on and responses to fire. An example would be semiarid and xeric shrublands as opposed to semiarid savannas. One biome is dominated by grasses, which results in differences in flammability and predisposition to fire. Importantly, xeric shrublands may be dominated by plant species that are obligate seeders, whereas semiarid savannas will be dominated by woody species that resprout after fire. Hence, the functional differences associated with biome are not well distinguished via currently available remotely sensed indexes of vegetation. The majority biome class for each 0.5° grid cell was used in the analysis.

Data Preparation. The analysis was run at 0.5° resolution for all half-degree grids for which there was fire information. Fire, climate, and vegetation variables were extracted for each 0.5° cell as discussed earlier. Where no FRP, burned area, or fire size data were recorded, points were excluded. There were a further 4,670 cells for which a CV of burned area could not be calculated because it returned the maximum CV possible—a value of 3.741657. These points were then also excluded. Values that fell within biomes classified as rock, ice, bare ground, sandy deserts, open water, mangrove, or tundra were also excluded. Cells known to be associated with high levels of volcanic activity were excluded, which included areas such as Iceland, Hawaii, and the Azores. We also excluded isolated points associated with regions of very high industrial activity, such as points that fell within Saudi Arabia, England, and Germany, and points that fell on small islands, such as the Andamans and small Pacific islands. Our final dataset contained 26,455 data points.

Spatial autocorrelation was not considered to be problematic in this analysis. It was very likely that points close in space would display similar fire regimes, but we were aiming to identify the boundaries between these different regions. Nevertheless, for all analyses, we used bootstrap methods or randomly selected training and testing datasets.

Principal Components Analysis and Biplots. A principal components analysis was run by using the princomp package in the R statistical package. Nonnormal data (FRI, FRP, CVBA, fire size) were logged, and all data were rescaled between 0 and 1 and centered. All five fire characteristics contributed significantly to the principal components and were largely orthogonal to each other (Fig. S4).

Biplots of each fire characteristic against the other four gives an indication of the constraints and tradeoffs between characteristics in multidimensional fire space (Fig. S3). The main text includes a detailed discussion of some of these constraints.

Model-Based Clustering Methods for Identifying Pyromes. The R statistical package Mclust was used to identify regions of similar fire regimes (i.e., pyromes). This package allows statistical comparison of different cluster sizes and the shapes of the clusters using the Bayesian information criterion (BIC). Importantly, it also allows for estimation of uncertainty around classifications by using expectation maximization methods (31), and for predicting the grouping of points not used in the original analysis based on their attributes.

We used a default prior with two clusters and a variable shape, variable volume, variable orientation model to regularize the fit to the data. An initial analysis using all possible parameterizations of the covariance matrix and cluster sizes from two to 15 indicated that a model with variable volume, shape, and orientation gave the best results (i.e., highest BIC)—which was unsurprising, as we did not expect our pyromes to be of similar size or inhabit similarly shaped fire space. Choosing the correct number of clusters (i.e., pyromes) was difficult because the BIC continued to increase to 15 clusters. Beyond five clusters, the increase in BIC was negligible (Fig. S5) and did not justify further splitting of the data.

Processor-constraints prevented us from running a clustering analysis on all 26,455 data points, so we selected a training sample of 10,900 points and predicted the pyrome of the remaining

approximately 15,000 points by using discriminant analysis (the mclustDAtrain and mclustDAtest functions in Mclust). These results showed high repeatability with different random selections of training and testing data. All points were ultimately classified into one of five pyromes with an associated uncertainty value. Uncertainties were fairly constant across pyromes, with most points having uncertainty values less than 0.2 (Fig. S6) and no clear spatial pattern emerging.

The clustering method used was not hierarchical—i.e., a new model was run each time we changed the number of clusters. It did appear, however, that there was some continuity in how the data were grouped as cluster size increased. The first split appeared to separate between frequent fires and infrequent fires (Fig. S7), and this was largely retained in the third split, whereby the infrequent fires were further split into those with short fire seasons and large burned areas (i.e., temperate regions) and those with long fire seasons and smaller burned areas (i.e., tropical regions). The four-cluster solution further split the temperate regions into low and high fireline intensities (i.e., crown fire and ground fire), and the five-cluster solutions split the frequent fire cluster (which had remained fairly unchanged) into a pyrome with small fires and one with large fires.

1. Giglio L, et al. (2010) Assessing variability and long-term trends in burned area by merging multiple satellite fire products. *Biogeosciences* 7:1171–1186.
2. Byram G (1959) *Forest Fire: Control and Use*, ed Davis K (McGraw Hill, New York), pp 61–89.
3. Keeley J (2009) Fire intensity, fire severity and burn severity: A brief review and suggested usage. *Int J Wildland Fire* 18:116–126.
4. Kaufman Y, et al. (1996) Relationship between remotely sensed fire intensity and rate of emission of smoke: SCAR-C experiment. *Global Biomass Burning*, ed Levine J (MIT Press, Cambridge, MA), pp 685–696.
5. Wooster M, Zhukov B, Oertel D (2003) Fire radiative energy for quantitative study of biomass burning: Derivation from the BIRD experimental satellite and comparison to MODIS fire products. *Remote Sens Environ* 86:83–107.
6. Roberts G, et al. (2005) Retrieval of biomass combustion rates and totals from fire radiative power observations: Application to southern Africa using geostationary SEVIRI imagery. *J Geophys Res* 110:D21111.
7. Smith A, Wooster M (2005) Remote classification of head and backfire types from MODIS fire radiative power and smoke plume observations. *Int J Wildland Fire* 14:249.
8. Giglio L, Loboda T, Roy D, Quayle B, Justice C (2009) An active-fire based burn area mapping algorithm for the MODIS sensor. *Remote Sens Environ* 113:408–420.
9. Archibald S, Scholes R, Roy D, Roberts G, Boschetti L (2010) Southern African fire regimes as revealed by remote sensing. *Int J Wildland Fire* 19:861–878.
10. Polakow D, Dunne T (1999) Modelling fire-return interval T: Stochasticity and censoring in the two-parameter Weibull model. *Ecol Modell* 121:79–102.
11. McCarthy M, Gill AM, Bradstock RA (2001) Theoretical fire-interval distributions. *Int J Wildland Fire* 10:73–77.
12. Moritz MA, Moody T, Miles L, Smith M, de Valpine P (2009) The fire frequency analysis branch of the pyrostatistics tree: Sampling decisions and censoring in fire interval data. *Environ Ecol Stat* 16:271–289.
13. Guyette RP, Stambaugh MC, Dey DC, Muzika RM (2012) Predicting fire frequency with chemistry and climate. *Ecosystems* 15:322–335.
14. Malamud BD, Morein G, Turcotte DL (1998) Forest fires: An example of self-organized critical behavior. *Science* 281(5384):1840–1842.
15. Strauss D, Bednar L, Mees R (1989) Do one percent of forest fires cause ninety-nine percent of the damage? *For Sci* 35:319–328.
16. Archibald S, Roy D (2009) Identifying individual fires from satellite-derived burned area data. *Proc IGARSS* 3:160–163.
17. Justice C, et al. (2011) Modis-derived global fire products. *Land Remote Sensing and Global Environmental Change*, eds Ramachandran B, Justice CO, Abrams MJ (Springer, Berlin), pp 661–679.
18. Balch J, Bradley B, D'Antonio C, Gómez-Dans J (2013) Introduced annual grass increases regional fire activity across the arid western USA (1980–2009). *Global Change Biology* 19:173–183.
19. Le Page Y, Oom D, Silva J, Jönsson P, Pereira J (2010) Seasonality of vegetation fires as modified by human action: Observing the deviation from eco-climatic fire regimes. *Glob Ecol Biogeogr* 19:575–588.
20. Archibald S, Roy D, Van Wilgen BW, Scholes RJ (2009) What limits fire?: An examination of the drivers of burnt area in southern Africa. *Glob Change Biol* 15:613–630.
21. Markham C (1970) Seasonality of precipitation in the United States. *Ann Assoc Am Geogr* 60:593–597.
22. Stott P (2000) Combustion in tropical biomass fires: A critical review. *Prog Phys Geogr* 24:355–377.
23. Bradstock RA (2010) A biogeographic model of fire regimes in Australia: Contemporary and future implications. *Glob Ecol Biogeogr* 19:145–158.
24. Stephenson NL (1998) Actual evapotranspiration and deficit: Biologically meanful correlates of vegetation distribution across spatial scales. *J Biogeogr* 25:855–870.
25. van der Werf GR, et al. (2004) Continental-scale partitioning of fire emissions during the 1997 to 2001 El Niño/La Niña period. *Science* 303(5654):73–76.
26. Swetnam TW, Betancourt JL (1990) Fire-southern oscillation relations in the southwestern United States. *Science* 249(4972):1017–1020.
27. Nepstad D, et al. (2004) Amazon drought and its implications for forest flammability and tree growth: A basin-wide analysis. *Glob Change Biol* 10:704–717.
28. Chuvieco E, Giglio L, Justice C (2008) Global characterization of fire activity: Toward defining fire regimes from earth observation data. *Glob Change Biol* 14: 1488–1502.
29. Aldersley A, Murray SJ, Cornell SE (2011) Global and regional analysis of climate and human drivers of wildfire. *Sci Total Environ* 409(18):3472–3481.
30. Sanderson E, et al. (2002) The human footprint and the last of the wild. *Bioscience* 52:891–904.
31. Fraley C, Raftery A (2007) Bayesian regularization for normal mixture estimation and model-based clustering. *J Classification* 24:155–181.

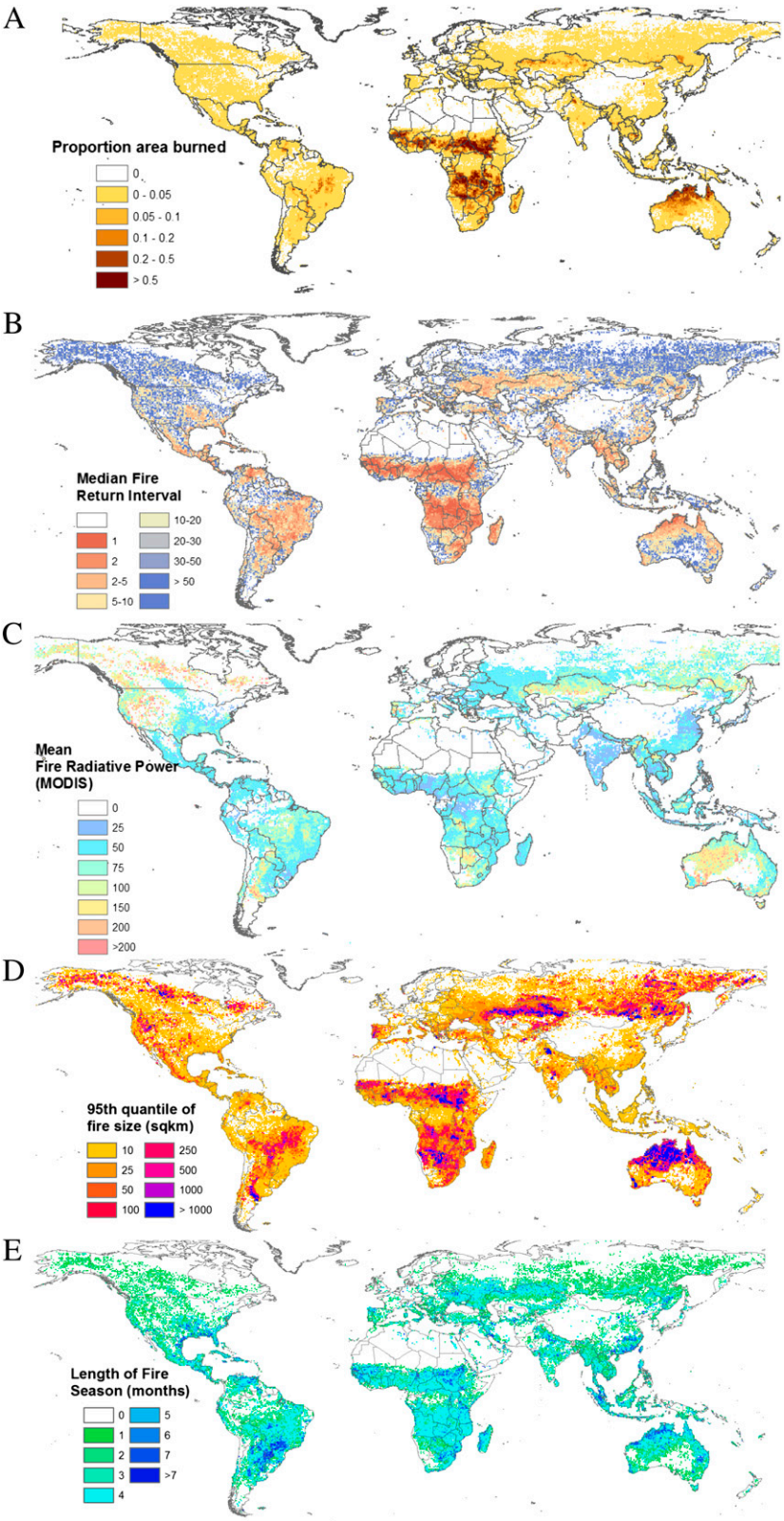

Fig. S1. Maps of the five fire characteristics used in the analysis. (*A*) Mean fraction of area burned. (*B*) Median fire return interval. (*C*) Mean fire radiative power. (*D*) Maximum (95th quantile) fire size. (*E*) Length of the fire season in months.

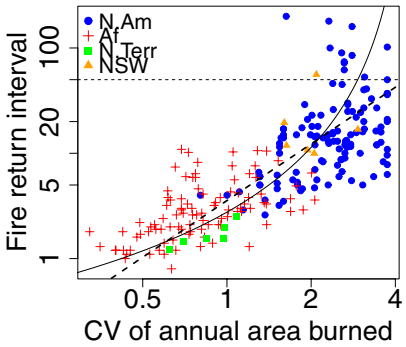

Fig. S2. Testing the relationship between CV of burned area and median FRI (in years) on four different validation datasets. The CVBA is a good predictor of FRI for FRI values less than 50 y. Above this value, the CVBA seems to saturate and gives a less accurate prediction. Lines represent a linear and a logistic model fit to the data (goodness-of-fit statistics reported in the text). Af, African FRI dataset from Archibald et al. (1); N.Am, North American FRI dataset from Guyette et al. (2); N.Terr, Arnhem Land dataset from the Northern Territory Department of Land Resource Management (from Bushfires Northern Territory); NSW, New South Wales dataset from New South Wales Office of Environment and Heritage and New South Wales Rural Fire Service fire history archives.

1. Archibald S, Scholes R, Roy D, Roberts G, Boschetti L (2010) Southern African fire regimes as revealed by remote sensing. *Int J Wildland Fire* 19:861–878.
2. Guyette RP, Stambaugh MC, Dey DC, Muzika RM (2012) Predicting fire frequency with chemistry and climate. *Ecosystems* 15:322–335.

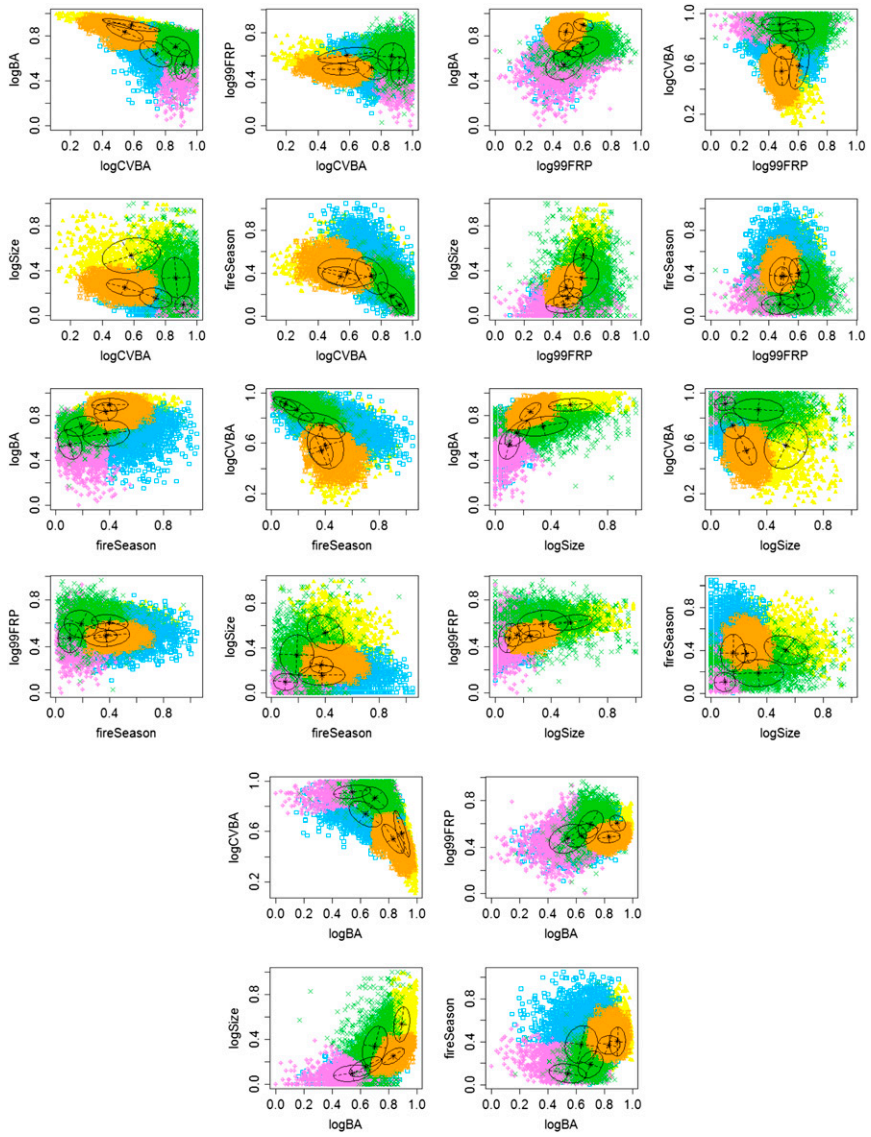

Fig. S3. Biplots of all fire characteristics against each other. The colors represent the five different pyromes identified by expectation–maximization clustering (yellow, frequent–intense–large; orange, frequent–cool–small; green, rare–intense–large; purple, rare–cool–small; blue, intermediate–cool–small) and the volumes of these five pyromes in 2D fire space are indicated with black stars (mean) and circles (1 SD). BA, burned area.

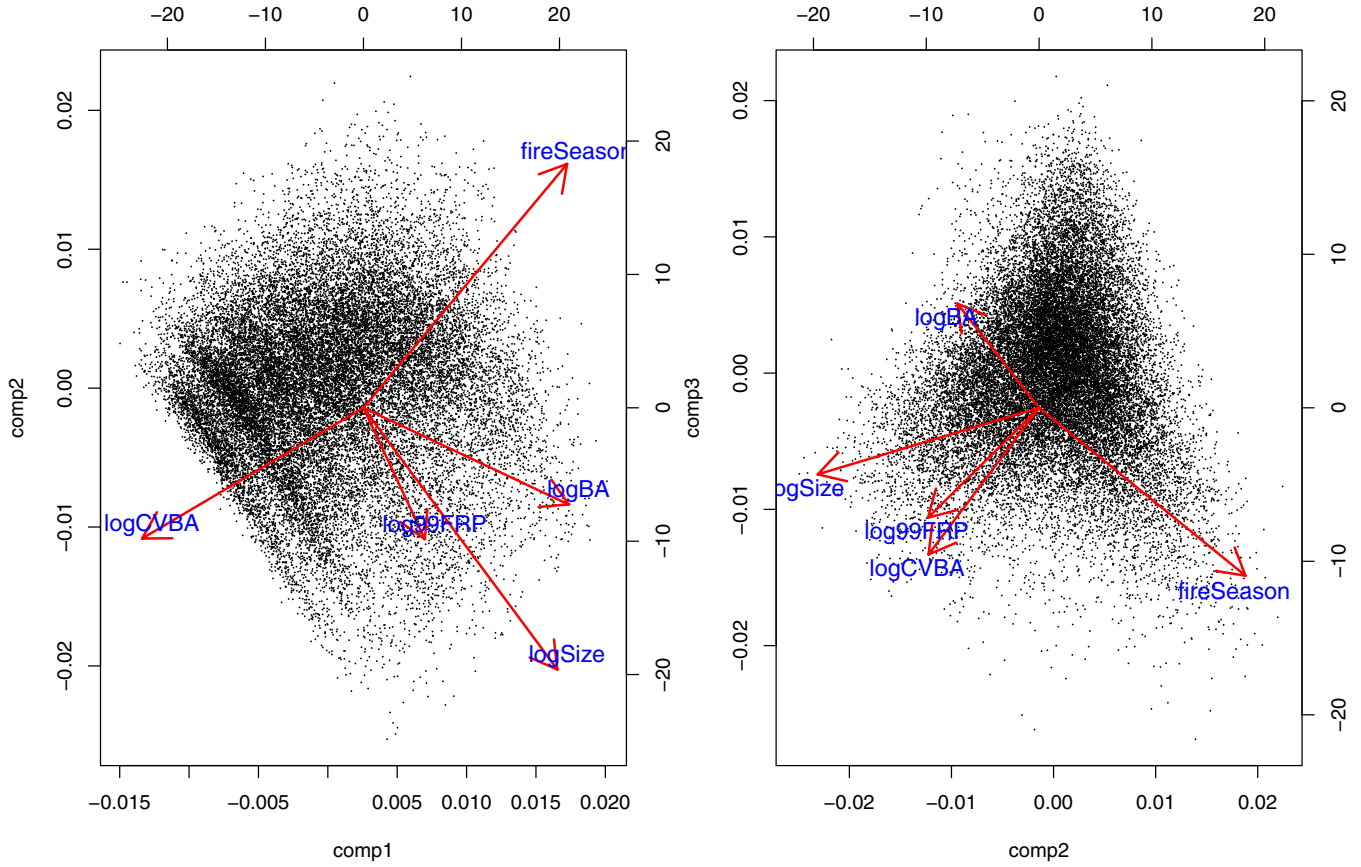

Fig. S4. Principal components analysis of the dimensions of variation of the five fire characteristics. This was used to identify the final five characteristics used in the analysis and to ensure that they represent important axes of variation in fire space.

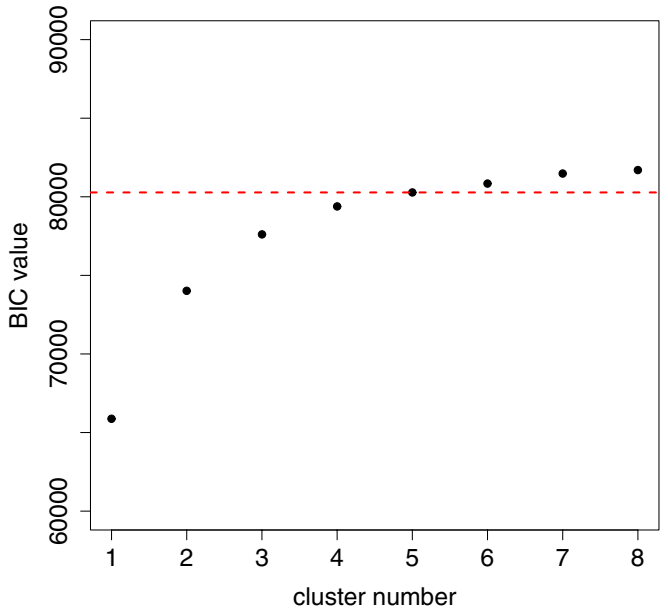

Fig. S5. Identification of the number of clusters (i.e., pyromes) by using BIC and expectation–maximization clustering.

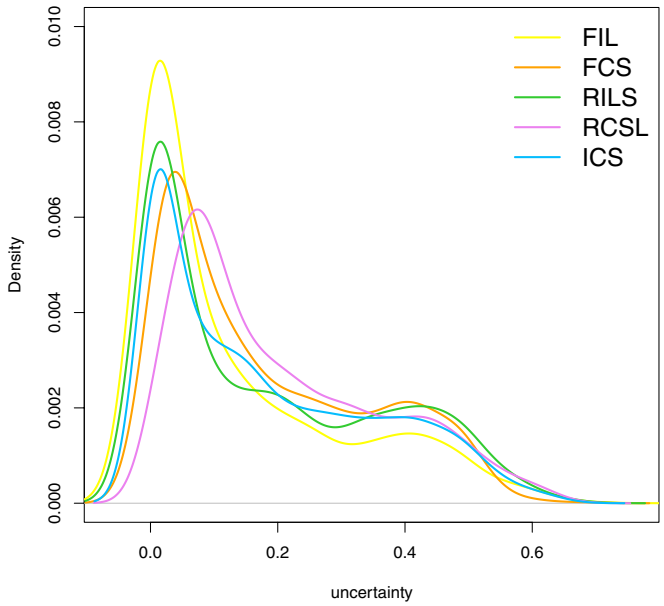

Fig. S6. Distribution of uncertainty values for the five different pyrome classes.

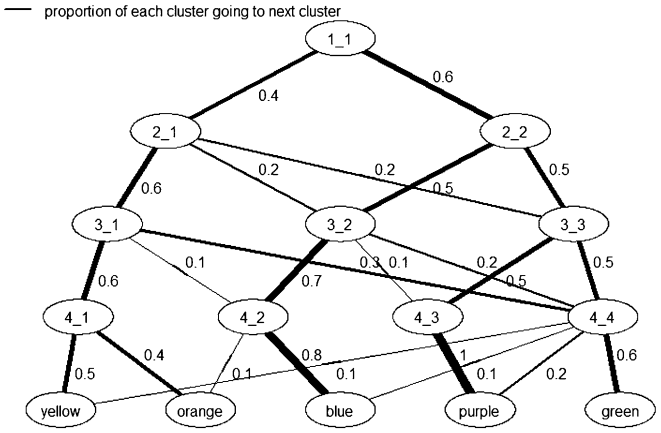

Fig. S7. Dendrogram showing how five pyromes emerge from clustering (clusters are not nested and five different analyses were run, one for each level). The fraction value and the thickness of the line show the proportion of points that moved between clusters at each level. The high-intensity crown fire regime (green) emerges in only the four-cluster solution. The frequent fire pyromes (yellow and orange) emerge in the two-cluster solution but are first distinguished from each other in the five-cluster solution. The blue/human fire regime is established in the three-cluster solution and remains fairly consistent from then onwards.

Table S1. Association between pyromes and biomes

Biome	FIL	FCS	RIL	RCS	ICS	FIL	FCS	RIL	RCS	ICS	Total
Tropical moist broadleaf forests	2	13	4	15	**26**	2	10	5	**28**	**56**	100
Tropical dry broadleaf forests	1	6	1	2	6	3	21	6	16	**53**	100
Tropical coniferous forests	0	1	1	1	2	0	10	13	17	**59**	100
Temperate mixed forests	1	2	6	17	16	1	2	11	**41**	**45**	100
Temperate coniferous forests	0	0	5	6	3	2	0	26	**45**	**26**	100
Boreal forests	1	0	**33**	**24**	2	1	0	**46**	**47**	6	100
Tropical grasslands	**58**	**67**	11	5	16	**29**	**33**	9	6	**23**	100
Temperate grasslands	11	4	14	13	14	10	3	**21**	**29**	**37**	100
Flooded grasslands	5	2	1	0	1	**46**	17	8	5	**24**	100
Montane grasslands	1	3	1	3	2	6	15	13	**31**	**36**	100
Mediterranean vegetation	0	1	4	4	3	1	3	**25**	**36**	**35**	100
Xeric vegetation	18	1	18	10	9	18	1	**31**	**24**	**26**	100
Total	100	100	100	100	100	NA	NA	NA	NA	NA	NA

Values on the left represent the proportion of each pyrome occupied by various biomes, values on the right the proportion of each biome occupied by various pyromes. Values greater than 20% are marked in bold. FCS, frequent–cool–small; FIL, frequent–intense–large; ICS, intermediate–cool–small; NA, not applicable; RCS, rare–cool–small; RIL, rare–intense–large.